

## Supramolecular Mn–Ca Aggregates as Models for the Photosynthetic Water Oxidation Complex

Sergiu M. Gorun,<sup>\*1a</sup> Robert T. Stibrany,<sup>1b</sup> and Antonietta Lillo<sup>1a</sup>

Chemistry Department, Brown University, Providence, Rhode Island 02912, and Exxon Research and Engineering, Annandale, New Jersey 08801

Received October 16, 1997

Tetranuclear manganese aggregates of yet unknown topology are the site of oxygen evolution in the water oxidizing complex (WOC) of photosystem II.<sup>2</sup> The WOC cycles through five oxidation states, S<sub>0</sub> to S<sub>4</sub>, during water oxidation. Calcium is essential for catalytic activity.<sup>3</sup> At least one Ca<sup>2+</sup> is believed<sup>4</sup> to be linked by a carboxylic acid residue to the Mn aggregate,<sup>5,6</sup> perhaps 3.3 Å from a Mn center<sup>7</sup> or, alternatively, at distances larger than 3.6 Å.<sup>8,9</sup> Ca<sup>2+</sup> can be replaced by alkaline-earth (AE) ions such as Sr<sup>2+</sup> and Ba<sup>2+</sup>, yielding lower activity.<sup>10–12</sup> The assembly of the Mn aggregate of WOC at Mn<sup>II</sup><sub>x</sub>Mn<sup>III</sup><sub>y</sub> oxidation level also requires Ca<sup>2+</sup>.<sup>13</sup> Ca<sup>2+</sup> depletion or replacement by Sr<sup>2+</sup> results in Mn magnetic interactions changes, as evidenced by variations in the ESR signal.<sup>10,14</sup> The structural basis for the above variability in WOC reactivity and spectroscopy is not clear.

Synthetic approaches to WOC models have focused mainly on building Mn complexes of various topologies and oxidation states.<sup>15</sup> Less attention has been paid to the incorporation of Ca cofactors in Mn aggregates. To our knowledge there are no structurally characterized di- or higher nuclearity Mn/Ca coordination complexes: only one, mononuclear complex, MnDPDP, with Ca<sup>2+</sup> (and Na<sup>+</sup>) counterions has been reported.<sup>16</sup> Ligands with terminal carboxylic groups offer the possibility of ligating

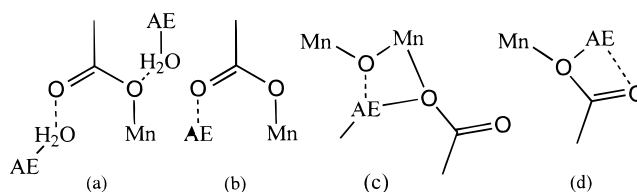


Figure 1. Examples of possible Mn–oxo–carboxylato/AE interactions.

additional alkaline-earth ions to Mn complexes as we demonstrated for a Mn<sub>4</sub>/BaCa aggregate.<sup>17</sup>

We report the synthesis and catalytic activity of the first example of a Mn<sub>4</sub>/Ca<sub>2</sub> aggregate and its Ba analogue, Mn<sub>4</sub>/Ba<sub>2</sub>. The above complexes form a complete series obtained by stepwise replacement of Ca by Ba cations in Mn<sub>4</sub>/alkaline-earth assemblies.

The synthesis<sup>18</sup> of [Mn<sup>III</sup><sub>3</sub>Mn<sup>II</sup>(μ-OHO)L<sub>2</sub>(O<sub>2</sub>CCH<sub>3</sub>)<sub>2</sub>](AE)<sub>2</sub>·xH<sub>2</sub>O where L is the pentaanion of 1,3-diamino-2-hydroxypropane-*N,N,N'*-tetraacetic acid and AE = Ca or Ba parallels the WOC assembly process, namely, oxidizing mixtures of Mn<sup>2+</sup> and AE salts of L in water at pH ~ 7.<sup>19</sup> No lower or higher oxidation level complexes were isolated, irrespective of the cation. The Mn(III)<sub>3</sub>Mn(II) level corresponds to either to the S<sub>0</sub><sup>20</sup> or S<sub>-2</sub><sup>7,21</sup> level of WOC.

The structures of the [Mn<sub>4</sub>(OHO)L<sub>2</sub>(O<sub>2</sub>CCH<sub>3</sub>)<sub>2</sub>]<sup>4-</sup> anions of **1** and **2** are shown in Figure 2. The previously reported Mn<sub>4</sub>/BaCa complex, **3**, isomorphous with **1**, is included for comparison in Figure S5. A crystallographically imposed mirror plane that passes through the OHO group renders two sets of Mn ions equivalent. The symmetry is broken in the BaBa complex, **2**, rendering the Mn nonequivalent while preserving their coordination geometry and ligand binding modes.

For both Mn(III,III) and Mn(III,II) pairs, the Mn–Mn distances vary in the order Ca<sub>2</sub> ≈ CaBa > BaBa. The Mn(III) ions, the Mn1, Mn1' pair of **1** and the corresponding Mn1, Mn3 pair of **2**, exhibit a rare Jahn–Teller compression geometry: average equatorial distances are 2.062(4) and 2.071(6) Å for **1** and **2**, respectively, while the average axial distances are 1.970(4) and 1.960(7) Å, respectively. A similar compression is observed for

- (1) (a) Brown University. (b) Exxon.
- (2) Recent major reviews: (a) Yachandra, V. K.; Sauer, K.; Klein, M. P. *Chem. Rev.* **1996**, *96*, 2927. (b) Debus, R. J. *Biochim. Biophys. Acta* **1992**, *1102*, 269. (c) Rutherford A. W.; Zimmermann, J.-L.; Boussac, A. In *The Photosystems: Structure, Function, and Molecular Biology*; Barber, J., Ed.; Elsevier: Amsterdam, 1992; pp 179–229. (d) Britt, R. D. In *Oxygenic Photosynthesis: The Light Reaction*; Ort, D. R., Yocum, C. F., Eds.; Kluwer: Dordrecht, 1996; pp 137–164.
- (3) Recent review: Yocum, C. F. In *Manganese Redox Enzymes*; Pecoraro, V. L., Ed.; VCH: New York, 1992; pp 71–83.
- (4) Ådelroth, P.; Lindberg, K.; Andréasson, L.-E. *Biochemistry* **1995**, *34*, 9021.
- (5) (a) Chen, C.; Kazimir, J.; Cheniae, G. M. *Biochemistry* **1995**, *34*, 13511. (b) Shen, J. R.; Satoh, K.; Katoh, S. *Biochim. Biophys. Acta* **1988**, *886*, 386.
- (6) Noguchi, T.; Ono, T.-A.; Inoue, Y. *Biochim. Biophys. Acta* **1995**, *1228*, 189.
- (7) (a) Latimer, M. J.; Yachandra, V. K.; Mukerji, I.; DeRose, V. J.; Sauer, K.; Klein, M. P. *Biochemistry* **1995**, *34*, 10898. (b) DeRose, V. J.; Mukerji, I.; Latimer, M. J.; Yachandra, V. K.; Sauer, K.; Klein, M. P. *J. Am. Chem. Soc.* **1994**, *116*, 5239. (c) Yachandra, V. K.; DeRose, V. J.; Latimer, M. J.; Mukerji, I.; Sauer, K.; Klein, M. P. *Science*, **1993**, *260*, 675.
- (8) (a) Riggs-Gelasco, P. J.; Mei, R.; Yocum, C. F.; Penner-Hahn, J. E. *J. Am. Chem. Soc.* **1996**, *118*, 2387. (b) Riggs-Gelasco, P. J.; Mei, R.; Ghanotakis, D. F.; Yocum, C. F.; Penner-Hahn, J. E. *J. Am. Chem. Soc.* **1996**, *118*, 2400. (c) MacLachlan, D. J.; Bratt, P. J.; Nugent, J. H. A.; Evans, M. C. W. *Biochim. Biophys. Acta* **1994**, *1186*, 186.
- (9) Hatch, C.; Grush, M.; Bradley, R.; LoBrutto, R.; Cramer, S.; Frash, W. *Photosynthesis* **1995**, *2*, 425.
- (10) Boussac, A.; Rutherford, A. W. *Biochemistry* **1988**, *27*, 3476.
- (11) Dismukes, G. C.; Ananyev, G. M. Personal communication.
- (12) Tamura, N.; Cheniae, G. In *Light-Energy Transduction in Photosynthesis: Higher Plants and Bacterial Models*; Stevens, S. E.; Bryant, D. A. Eds.; The American Society of Plant Physiologists: Rockville, MD, 1988; pp 227–242.
- (13) (a) Ananyev, G. M.; Dismukes, G. C. *Biochemistry* **1996**, *35*, 14608. (b) Ananyev, G. M.; Dismukes, G. C. *Biochemistry* **1997**, *36*, 11342. (c) Zaltsman, L.; Ananyev, G. M.; Bruntrager, E.; Dismukes, G. C. *Biochemistry* **1997**, *36*, 8914.
- (14) Boussac, A.; Zimmerman, J.; Rutherford, A. W. *Biochemistry* **1989**, *28*, 8984.
- (15) Rüttinger, W.; Dismukes, G. C. *Chem. Rev.* **1997**, *97*, 1.

- (16) (a) DPDP is *N,N'*-dipyridoxylethylenediamine-*N,N'*-diacetate 5,5'-bis-(phosphate); Rocklage, S. M.; Cacheris, W. P.; Quay, S. C.; Hahn, F. E.; Raymond, K. N. *Inorg. Chem.* **1989**, *28*, 477. (b) Dinuclear Mn/Ca compositions of yet unknown structures have been reported: Horwitz, C. P.; Warden, J. T.; Weintraub, S. T. *Inorg. Chim. Acta* **1996**, *246*, 311. Their ESR spectra are unaffected by Ca, suggesting absence of direct linkages to the Mn center.
- (17) (a) Stibrany, R. T.; Gorun, S. M. *Angew. Chem., Int. Ed. Engl.* **1990**, *29*, 1156. (b) Stibrany, R. T.; Gorun, S. M. In *Dioxygen Activation and Homogeneous Catalytic Oxidation*; Simandi, L. I., Ed.; Elsevier: New York, 1991; pp 681–687. (c) Initial catalytic rates at 25 °C (L of O<sub>2</sub>/s/mol of catalyst) for **1–3** are 0.8, 1.3, and 1.4 (see Figure S1b).
- (18) **1** and **2** were prepared by using only Ca or Ba in the procedure of ref 17. X-ray quality crystals were obtained by the slow evaporation of the solvent. *Caution*: heat and O<sub>2</sub> evolve upon oxidations with H<sub>2</sub>O<sub>2</sub>.
- (19) See Supporting Information for EPR and other data.
- (20) (a) Zheng, M.; Dismukes, G. C. *Inorg. Chem.* **1996**, *35*, 3307. (b) Kusunoki, M.; Ono, T.-A.; Matsushita, T.; Oyanagi, H.; Inoue, Y. *J. Biochem.* **1990**, *108*, 560.
- (21) Riggs, P. J.; Mei, R.; Yocum, C. F.; Penner-Hahn, J. E. *J. Am. Chem. Soc.* **1992**, *114*, 10650.

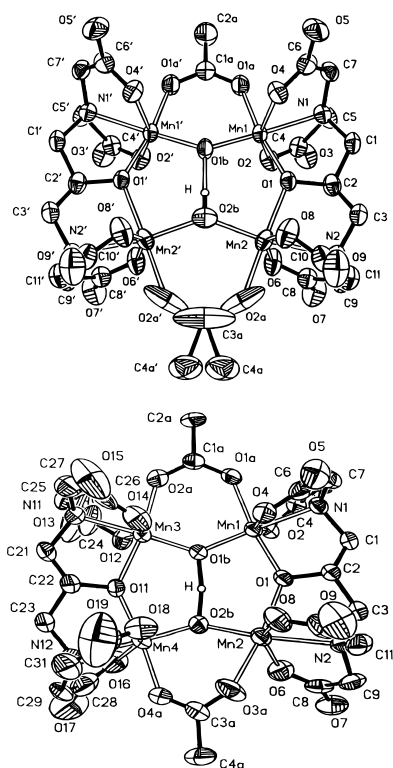


**Figure 2.** ORTEP plots of the anions of **1** (top) and **2** (bottom) and selected bond distances (Å) and angles (deg). **1**: Mn1–Mn1', 3.382(1); Mn1–Mn2, 3.726(1); Mn2–Mn2', 3.580; Mn1–O1b, 1.819(2); Mn2–O2b, 1.926(3); Mn1–O1b–Mn1', 136.7(3); Mn2–O2b–Mn2', 136.7(4); O1b–H–O2b, 180(7). **2**: Mn1–Mn2, 3.829(2); Mn1–Mn3, 3.315(2); Mn2–Mn4, 3.495(2); Mn3–Mn4, 3.712(2); Mn1–O1b, 1.854(5); Mn2–O2b, 2.069(5); Mn3–O1b, 1.817(5); Mn4–O2b, 1.848(5); Mn1–O1b–Mn3, 129.1(3); Mn2–O2b–Mn4, 126.2(2); O1b–H–O2b, 168(7).

Mn4 of **2** (eq 2.064(6) Å, axial 1.965(8) Å), but Mn2 bond distances are uniformly longer ( $\langle \text{Mn–ligand} \rangle = 2.186(6)$  Å), typical for Mn(II). The crystallographically equivalent Mn2-, Mn2' in **1** exhibit, as expected, average Mn(II), Mn(III) distances. Both **1** and **2** appear thus to be valence-localized complexes, similar to **3**, independent of the counterions. In **1**, which is similar to **3**, two hydrated Ca<sup>2+</sup> ions are bonded via H<sub>2</sub>O to terminal carboxylate groups (type "a", Figures 1 and S4). Mn–Ca distances range from 4.895 to 6.173 Å. The two Ca<sup>2+</sup> ions, bridged by water molecules, are *symmetrically* linked to both the Mn(III,III) and Mn(III,II) sides of the complex (Figures S2 and S4). A similar dinuclear Ca unit is present below the Mn<sub>4</sub> plane. In contrast, the Ba<sup>2+</sup> ions in **2** are directly (type "c") coordinated to terminal carboxylate oxygens: Ba1 is *asymmetrically* bonded above the Mn<sub>4</sub> plane on the Mn(III,III) side while disordered Ba2 is bonded to all four oxygens below the Mn<sub>4</sub> plane (Figures S3 and S4). This direct coordination leads, as expected, to shorter Ba–Mn distances, the shortest ones being: Ba1–Mn1, = 3.941 and Ba1–Mn3 = 3.879 Å.

Interestingly, *theoretical* replacement of Ba<sup>2+</sup> by Ca<sup>2+</sup> in **2** (coordination numbers of  $7 \pm 1$ ) results,<sup>22</sup> *inter alia*, in a short,

$3.56 \pm 0.03$  Å, type "c" (Figure 1) Ca–Mn(III) contact, shorter than a postulated Mn–Ca vector of 3.7 Å<sup>8c</sup> but slightly longer than the 3.3–3.5 Å EXAFS shell in WOC. If Mn(IV) is considered, a Ca–Mn(IV) distance of  $3.45 \pm 0.03$  Å is computed,<sup>22</sup> consistent with the 3.3–3.5 Å range. The 3.56 Å distance is, however, significantly shorter than the 4.3 Å, type "b", and 4.4 Å, type "d", Mn–Ca separations observed in concanavalin A<sup>23</sup> and Mn DPDP,<sup>16</sup> respectively. *Experimental* replacement of Ca<sup>2+</sup> by Ba<sup>2+</sup> results in a type "a" to "c" coordination transition accompanied by loss of overall symmetry. The  $\mu$ -OHO ligand, in particular (see Figure S4), changes from  $\mu_4$ -O1b–H–O2b (*symmetric*) to  $\mu_5$ -OHO ( $\mu_3$ -O1b +  $\mu_2$ -O2b) (*asymmetric*), by forming an unprecedented  $\mu_3$ -oxo bridged Mn<sub>2</sub>Ba motif (Ba–O1b = 3.040(5) Å). Such motifs have been postulated to occur in the S<sub>1</sub> state of WOC.<sup>13b</sup> Furthermore, the OHO group geometry appears to be AE dependent: H is perhaps closer to O1b than O2b (1.2(1) vs 1.3(1) Å) in **3**, closer to O2b than O1b (1.24(8) vs 1.34(8) Å) in **2**, but asymmetrically bonded, 1.6(1) from O1b vs 0.9(1) Å from O2b, in **1**. The O1b...O2b distances also vary slightly, from ~2.40 to 2.56 Å, in the order CaCa  $\approx$  CaBa < BaBa.

Ca<sup>2+</sup> substitution by Ba<sup>2+</sup> also affects the way other ligands bind to the Mn center. Acetates that bridge the Mn(III,III) pair in **1**, **2** and **3** exhibit similar coordination. In contrast, the one bridging the Mn(II,III) pair, which coordinates normally in **2** (Ba<sub>2</sub>), is somewhat disordered in **3** (BaCa) but severely so in **1** (CaCa): two CH<sub>3</sub> groups, C<sub>4a</sub> and C<sub>4a'</sub>, can be resolved in **1** (see Figure 2) despite similar average Mn–OAc distances of 2.078(5), 2.056(6), and 2.061(6) Å for **3**, **2**, and **1**, respectively. The disorder (asymmetric bridging) might be attributed to a combination of symmetry imposed averaging of the Mn(II)– and Mn(III)–OAc bonds (in **1** and **3**) and to *selective*, alkaline-earth ion-induced, lability of acetate–Mn bonds at the dinuclear Mn(II,III) site.

Isomorphous, stepwise, replacement of Ca<sup>2+</sup> by Ba<sup>2+</sup> thus results in relatively small *structural* changes in the Mn<sub>4</sub> core, despite significant changes in the alkaline-earth–Mn<sub>4</sub>–oxo supramolecular aggregate topologies. Both the Mn oxidation states and their valence-trapped nature, as well as the type of Jahn–Teller distortions, are also invariant with respect to substitution.<sup>19</sup> Both **1** and **2**, which retain their nuclearity in solution,<sup>24</sup> exhibit catalase activity similar to that of **3**,<sup>17</sup> **1** thus being the first example of a biomimetic Mn<sub>4</sub>/Ca model. The catalytic functions of **1** may parallel that of WOC, although the Mn origin of the latter has been challenged.<sup>25</sup>

The structures of **1**, **2**, and **3** reveal possible functional and structural roles for AE ions in WOC (AE-type dependent): (i) assistance in deprotonation of similar Mn-bonded  $\mu_4$ -OH<sub>x</sub>O groups which might form in WOC and which may<sup>17,26,27</sup> (or may not<sup>28</sup>) yield dioxygen; assisted deprotonation favors O–O coupling due to oxidation potential depression ( $\sim 0.26$  V/H<sup>+</sup> for H<sub>2</sub>O<sup>15a,29</sup>); (ii) stabilization of developing negative charges on deprotonated oxo species (cf.  $\mu_3$ -oxo Mn<sub>2</sub>Ba) which may regulate oxidation changes; (iii) "gate keeping" functions<sup>30</sup> based upon variable hydration numbers (Ca<sup>2+</sup> > Ba<sup>2+</sup>) and Ca positioning above/below Mn active site (Fig. S2 and S3<sup>24</sup>). The variability observed in oxo and carboxylate binding suggests that related AE-dependent structural changes may occur in WOC via similar (Figure 1) AE/carboxylato/oxo groups interactions.

**Acknowledgment.** We thank Drs. C. Day, S. Walton, S. L. Mullen, and H. Freund for X-ray, elemental analysis, MS, and TGA/MS data, respectively. FAB MS were obtained at the University of Illinois, supported by an NIGMS grant (GM 27029).

**Supporting Information Available:** ORTEP drawings and crystallographic, EPR, FAB, stability, and oxygen evolution data (48 pages). Ordering information is given on any current masthead page.

(22) Ionic radii from: Shannon, R. D. *Acta Crystallogr.* **1976**, A32, 751.

(23) Hardman, K. D.; Agarwal, R. C.; Freiser, M. J. *J. Mol. Biol.* **1982**, 157, 69.

(24) See the Supporting Information.

(25) Sheptovitsky, Y. G.; Brudvig, G. W. *Biochemistry* **1996**, 35, 16255.

(26) Proserpio, D. M.; Hoffmann, R.; Dismukes, G. C. *J. Am. Chem. Soc.* **1992**, 114, 4374.

(27) Gelasco, A.; Askenas, A.; Pecoraro, V. L. *Inorg. Chem.* **1996**, 35, 1419.

(28) Proserpio, D. M.; Rapé, A. K.; Gorun, S. M. *Inorg. Chim. Acta* **1993**, 213, 319.

(29) Krishtalik, L. I. *Biophysics* **1989**, 34, 958.

(30) Tso, J.; Sivaraja, M.; Dismukes, G. C. *Biochemistry* **1991**, 30, 4734.